SIAM J. SCI. COMPUT.
Vol. 42, No. 3, pp. B630–B655

THE EXPONENTIAL SCALAR AUXILIARY VARIABLE (E-SAV) APPROACH FOR PHASE FIELD MODELS AND ITS EXPLICIT COMPUTING*

ZHENGGUANG LIU† AND XIAOLI LI‡

Abstract. In this paper, we consider an exponential scalar auxiliary variable (E-SAV) approach to obtain energy stable schemes for a class of phase field models. This novel auxiliary variable method based on the exponential form of the nonlinear free energy potential is more effective and applicable than the traditional SAV method, which is very popular in constructing energy stable schemes. The first contribution is that the auxiliary variable without square root removes the bounded-from-below restriction of the nonlinear free energy potential. Then we prove the unconditional energy stability for semidiscrete schemes carefully and rigorously. Another contribution is that we provide a total and explicit discretization of the auxiliary variable combined with the nonlinear term. Such a modification is very efficient for fast calculations. Furthermore, the positivity preserving property of r can be guaranteed, which is very important and reasonable for the models' equivalence. In addition, for complex phase field models with two or more unknown variables and nonlinear terms, we construct a multiple E-SAV (ME-SAV) approach to enhance the applicability of the proposed E-SAV approach. A comparative study of classical SAV and E-SAV approaches is considered to show the accuracy and efficiency. Finally, we present various 2D numerical simulations to demonstrate the stability and accuracy.

Key words. phase field models, scalar auxiliary variable, exponential form, energy stability, numerical simulations

AMS subject classifications. 65M12, 35K20, 35K35, 35K55, 65Z05

DOI. 10.1137/19M1305914

1. Introduction.

Phase field models are very important equations in physics, material science, and mathematics [2, 14, 19, 20, 21, 27, 31, 32]. They have been widely used in many fields such as alloy casting, new material preparation, image processing, finance, and so on. Phase field models can simulate many physical phenomena, such as the formation process of snowflakes, the dendrite structure formed by water freezing, and the cellular or dendrite structure formed in the welding process. They are helpful in understanding the nature and the formation mechanism of various materials and the preparation of new materials. They are also of great practical significance in the development of new technologies.

In general, mathematically, phase field models are always derived from the functional variation of free energy, which can be written explicitly as follows [25]:

$$E(\phi) = (\phi, \mathcal{L}\phi) + E_1(\phi) = (\phi, \mathcal{L}\phi) + \int_\Omega F(\phi) d\mathbf{x}, \tag{1.1}$$

where $\mathcal{L}$ is a symmetric nonnegative linear operator and $E_1(\phi)$ is nonlinear but with derivatives of lower order compared to $\mathcal{L}$. $F(x)$ is the energy density function.

*Submitted to the journal's Computational Methods in Science and Engineering section December 10, 2019; accepted for publication (in revised form) March 2, 2020; published electronically May 13, 2020.

https://doi.org/10.1137/19M1305914

Funding: This work was supported by the China Postdoctoral Science Foundation under grants BX20190187 and 2019M650152, and by the National Natural Science Foundation of China under grants 11901489 and 11971276. No potential conflict of interest was reported by the authors.

†Corresponding author. School of Mathematics and Statistics, Shandong Normal University, Jinan, China (liuzhgsdu@yahoo.com).

‡Fujian Provincial Key Laboratory on Mathematical Modeling and High Performance Scientific Computing and School of Mathematical Sciences, Xiamen University, Xiamen, Fujian, 361005, China (xiaolisdu@163.com).

Phase field models from the energetic variation of the above energy functional $E(\phi)$ can be obtained as follows:

$$\frac{\partial \phi}{\partial t} = \mathcal{G}\frac{\delta E}{\delta \phi}, \tag{1.2}$$

where $\frac{\delta E}{\delta \phi}$ is variational derivative, and $\mathcal{G}$ is a nonpositive operator. For example, $\mathcal{G} = -I$ for the Allen–Cahn-type system and $\mathcal{G} = \Delta$ for the Cahn–Hilliard-type system for the Ginzburg–Landau double-well-type potential F. The system satisfies the following energy dissipation law naturally:

$$\frac{d}{dt}E = \left(\frac{\delta E}{\delta \phi}, \frac{\partial \phi}{\partial t}\right) = \left(\mathcal{G}\frac{\delta E}{\delta \phi}, \frac{\delta E}{\delta \phi}\right) \leq 0.$$

The energy dissipation law is a very important property for phase field models in physics and mathematics. Thus, this property is essential for numerical schemes. That is to say, the discrete energy of the proposed numerical discrete schemes should also maintain dissipative properties. Up to now, many scholars considered a series of efficient and popular time discretization approaches to construct energy stable schemes for phase field models such as the semi- or fully implicit approach [7, 34], the convex splitting approach [12, 22, 28], the linear stabilized approach [26, 39], the exponential time differencing (ETD) approach [9, 30], invariant energy quadratization (IEQ) approach [4, 5, 35], the scalar auxiliary variable (SAV) approach [15, 16, 24, 25], and so on. Specifically, the convex splitting method leads to a convex minimization problem at each time step, and the scheme is unconditionally energy stable and uniquely solvable. But it still needs to solve a nonlinear system, and it is difficult to construct a higher-order scheme. The linear stabilized method can effectively solve a linear system of phase field models, but the additional stabilized term leads to additional errors, which makes it difficult to construct the higher-order scheme. Both the IEQ and SAV methods are unconditional energy stabilization methods which have been developed in recent years. The IEQ method was inspired by the Lagrange multiplier method but makes a big leap. By introducing an auxiliary variable, X, Yang et al. [40, 38] successfully avoided the difficulty of discretization of the nonlinear term. The IEQ approach has been proven to keep many advantages such as the linear, easy-to-obtain second-order scheme and unconditional energy stability. This method has been successfully applied to numerical simulation for many complex phase field models. The SAV method was proposed by Shen and his collaborators [24, 25] and is another very popular and efficient approach. It is worth mentioning that the SAV method keeps all the advantages of the IEQ approach. Furthermore, it weakens the assumptions of the bounded-below restriction of the nonlinear free energy potential, which makes it a new important method for simulating the phase field models.

The first main contribution of this paper is that we find a proper way to get rid of the assumption of the nonlinear free energy potential in the SAV approach. In order to show and give a comparative study for our novel E-SAV approach, we provide below a brief review of the SAV approach to construct energy stable schemes for phase field models. In general, the phase field models (1.2) can always be written as the following by denoting the chemical potential $\mu = \frac{\delta E}{\delta \phi}$:

$$\begin{cases} \dfrac{\partial \phi}{\partial t} = \mathcal{G}\mu, \\ \quad \mu = \mathcal{L}\phi + F'(\phi), \end{cases}$$

subject to periodic boundary conditions or $\frac{\partial \phi}{\partial \mathbf{n}}|_{\partial\Omega} = \frac{\partial \mu}{\partial \mathbf{n}}|_{\partial\Omega} = 0$.

The key to the SAV approach is to transform the nonlinear potential into a simple quadratic form. This transformation makes the nonlinear term much easier to handle. Assume that $E_1(\phi)$ is bounded from below, which means that there exists a constant C to make $E_1(\phi) + C > 0$. Define a scalar auxiliary variable

$$r(t) = \sqrt{E_1(\phi) + C} = \sqrt{\int_\Omega F(\phi) d\mathbf{x} + C} > 0.$$

Then the nonlinear functional $F'(\phi)$ can be transformed into the following equivalent formulation:

$$F'(\phi) = \frac{r}{r} F'(\phi) = \frac{r}{\sqrt{E_1(\phi) + C}} F'(\phi).$$

Thus, an equivalent system of phase field models with scalar auxiliary variable can be rewritten as follows:

$$\begin{cases} \dfrac{\partial \phi}{\partial t} = \mathcal{G}\mu, \\ \mu = \mathcal{L}\phi + \dfrac{r}{\sqrt{E_1(\phi) + C}} F'(\phi), \\ r_t = \dfrac{1}{2\sqrt{E_1(\phi) + C}} \displaystyle\int_\Omega F'(\phi)\phi_t d\mathbf{x}. \end{cases} \tag{1.3}$$

Taking the inner products of the above equations with μ, ϕ_t, and $2r$, respectively, we obtain that the above equivalent system satisfies a modified energy dissipation law:

$$\frac{d}{dt}\left[\frac{1}{2}(\phi, \mathcal{L}\phi) + r^2\right] = (\mathcal{G}\mu, \mu) \le 0. \tag{1.4}$$

Remark 1.1. Define $E(\phi, r) = \left[\frac{1}{2}(\phi, \mathcal{L}\phi) + r^2\right]$. It is not difficult to notice that

$$E(\phi, r) = \frac{1}{2}(\phi, \mathcal{L}\phi) + E_1(\phi) + C = E(\phi) + C,$$

which means $E(\phi, r) \neq E(\phi)$ for $C \neq 0$. That is to say, for the SAV-based method, if the auxiliary variable $r(t)$ is defined as $r(t) = \sqrt{E_1(\phi) + C}$ and $C \neq 0$, then the energy stability is derived for a modified energy $E(\phi, r)$, not for the original energy functional $E(\phi)$.

With the above phase field models with the SAV scheme (1.3), it is very easy to construct linear, second-order, and unconditionally energy stable schemes. For example, a second-order semidiscrete scheme based on the Crank–Nicolson method reads as follows:

$$\begin{cases} \dfrac{\phi^{n+1} - \phi^n}{\Delta t} = \mathcal{G}\mu^{n+1/2}, \\ \mu^{n+1/2} = \mathcal{L}\left(\dfrac{\phi^{n+1} + \phi^n}{2}\right) + \dfrac{r^{n+1} + r^n}{2\sqrt{E_1(\tilde{\phi}^{n+1/2}) + C}} F'(\tilde{\phi}^{n+1/2}), \\ \dfrac{r^{n+1} - r^n}{\Delta t} = \dfrac{1}{2\sqrt{E_1(\tilde{\phi}^{n+1/2}) + C}} \displaystyle\int_\Omega F'(\tilde{\phi}^{n+1/2}) \frac{\phi^{n+1} - \phi^n}{\Delta t} d\mathbf{x}, \end{cases} \tag{1.5}$$

where $\tilde{\phi}^{n+\frac{1}{2}}$ is any explicit $O(\Delta t^2)$ approximation for $\phi(t^{n+\frac{1}{2}})$, which can be flexible according to the problem.

It is not difficult to prove that the above scheme is unconditionally energy stable in the sense that

$$\left[\frac{1}{2}(\mathcal{L}\phi^{n+1},\phi^{n+1})+|r^{n+1}|^2\right]-\left[\frac{1}{2}(\mathcal{L}\phi^{n},\phi^{n})+|r^{n}|^2\right]\le \Delta t(\mathcal{G}\mu^{n+1/2},\mu^{n+1/2})\le 0.$$

The SAV approach has been treated as a very efficient and powerful way of constructing energy stable schemes, and it is easy to calculate. However, there is one obvious shortcoming: the models need to satisfy an assumption that the nonlinear free energy $E_1(\phi)$ is bounded from below. In order to ensure the correctness of the discrete scheme, we have to give a very big positive C before calculation. However, it is observed that the C value seems to have an influence on the accuracy of the simulation results. Relative study can be found in [18], which found that the error histories for $C = 0.01$ and $C = 500$ exhibit quite different characteristics. The error corresponding to C decreases quickly, but the error corresponding to $C = 500$ decreases extremely slowly at this stage. To enhance the applicability of the SAV method, we aim to find a reasonable procedure to avoid using an estimated number C during the calculation. We consider an E-SAV method by using the constant positive properties of exponential functions to obtain energy stable schemes. We prove the unconditional energy stability for the semidiscrete schemes carefully and rigorously.

The second contribution is that the discrete scheme based on the E-SAV approach makes it very easy to construct explicit numerical scheme. Such a modification is very efficient for fast calculation. In addition, for complex phase field models with two or more unknown variables and nonlinear terms, we construct a multiple E-SAV (ME-SAV) approach to enhance the applicability of the proposed E-SAV approach. A comparative study of classical SAV and E-SAV approaches is considered to show the accuracy and efficiency. Finally, we present various 2D numerical simulations to demonstrate the stability and accuracy.

In summary, the constructed E-SAV approach has the following five advantages compared with the recently proposed SAV approach:

(i) The E-SAV approach does not need any assumptions, while the nonlinear free energy potential has to be bounded from below in the SAV approach.

(ii) The novel auxiliary variable r and r^n are always positive in E-SAV schemes. However, such a positive property of r^n cannot be guaranteed in the SAV approach.

(iii) Totally explicit energy stable schemes can be easily constructed by using our E-SAV approach, while such explicit schemes cannot preserve the energy dissipation law for the SAV approach.

(iv) The computations of ϕ^{n+1} and the auxiliary variable r^{n+1} can be solved step by step based on the E-SAV approach, while we have to compute an inner product before calculating ϕ^{n+1} in the SAV schemes.

(v) Schemes based on the E-SAV approach dissipate the original energy, as opposed to a modified energy in the SAV approach.

The paper is organized as follows. In section 2, we introduce the E-SAV approach for phase field models and give two numerical discrete schemes. Then we prove unconditional energy stability for the semidiscrete scheme. In section 3, the E-SAV approach of the phase field models of several functions is considered. In section 4, considering that the exponential function is a rapidly increasing function which carries the risk of failure for the E-SAV approach, we give a modified technique to improve the scope of application. To enhance the applicability of the proposed E-SAV ap-

proach for complex phase field models, we construct a multiple E-SAV approach in section 5. Finally, in section 6, various 2D numerical simulations are demonstrated to verify the accuracy and efficiency of our proposed schemes.

2. E-SAV approach for phase field models. In this section, we will consider an E-SAV approach for phase field models to construct energy stable numerical schemes. The exponential function is a special function that keeps the range constant positive. Thus, we introduce an exponential scalar auxiliary variable (E-SAV):

$$r(t) = \exp\left(E_1(\phi)\right) = \exp\left(\int_\Omega F(\phi) d\mathbf{x}\right). \tag{2.1}$$

It is obvious that $r(t) > 0$ for any t. Then the nonlinear functional $F'(\phi)$ can be transformed into the following equivalent formulation:

$$F'(\phi) = \frac{r}{r} F'(\phi) = \frac{r}{\exp\left(E_1(\phi)\right)} F'(\phi).$$

By taking the derivative of (2.1) with respect to t and replacing $F'(\phi)$ with the above expression, we obtain

$$\frac{dr}{dt} = r \int_\Omega F'(\phi)\phi_t d\mathbf{x} = \frac{r^2}{\exp\left(E_1(\phi)\right)} \int_\Omega F'(\phi)\phi_t d\mathbf{x}.$$

Thus, (1.5) can be rewritten as the following equivalent system:

$$\begin{cases} \dfrac{\partial \phi}{\partial t} = \mathcal{G}\mu, \\ \quad \mu = \mathcal{L}\phi + \dfrac{r}{\exp\left(E_1(\phi)\right)} F'(\phi), \\ \quad r_t = \dfrac{r^2}{\exp\left(E_1(\phi)\right)} \displaystyle\int_\Omega F'(\phi)\phi_t d\mathbf{x}. \end{cases} \tag{2.2}$$

To simplify the notation, we define

$$b^{r,\phi} = \frac{r}{\exp\left(E_1(\phi)\right)} F'(\phi).$$

Then the above system (2.2) can be transformed as follows:

$$\begin{cases} \dfrac{\partial \phi}{\partial t} = \mathcal{G}\mu, \\ \quad \mu = \mathcal{L}\phi + b^{r,\phi}, \\ \quad r_t = r(b^{r,\phi}, \phi_t). \end{cases} \tag{2.3}$$

Taking the inner products of the first two equations with μ and ϕ_t in (2.3), respectively, we obtain that

$$\left(\frac{\partial \phi}{\partial t}, \mu\right) = (\mathcal{G}\mu, \mu) \le 0 \tag{2.4}$$

and

$$\left(\frac{\partial \phi}{\partial t}, \mu\right) = \frac{1}{2}\frac{d}{dt}(\mathcal{L}\phi, \phi) + (b^{r,\phi}, \phi_t). \tag{2.5}$$

For the third equation in (2.3), noting that $r > 0$, it can then be transformed as follows:

$$\frac{d\ln(r)}{dt} = (b^{r,\phi}, \phi_t). \tag{2.6}$$

Combining (2.4)–(2.5) with (2.6), we obtain the following energy dissipation law:

$$\frac{d}{dt}\left[\frac{1}{2}(\mathcal{L}\phi,\phi) + \ln(r)\right] = (\mathcal{G}\mu,\mu) \le 0.$$

Remark 2.1. For the SAV approach in (1.5), the modified energy dissipation law is not equal to the original one because of $\left[\frac{1}{2}(\mathcal{L}\phi^n,\phi^n) + |r^n|^2\right] = E(\phi) + C$. However, notice that $\ln(r) = \ln(\exp(E_1(\phi))) = E_1(\phi)$. Thus, we have $\frac{1}{2}(\mathcal{L}\phi,\phi) + \ln(r) = E(\phi)$, which means the above energy inequality is totally equal to the original energy dissipation law.

Next, we will consider some numerical schemes to illustrate that with the proposed E-SAV approach, it is very easy to obtain linear and unconditionally energy stable schemes. More importantly, it can be found that both first-order and second-order explicit numerical schemes with unconditionally energy stability can be constructed easily.

Before giving a semidiscrete formulation, we let $N > 0$ be a positive integer and set

$$\Delta t = T/N, \quad t^n = n\Delta t \quad \text{for} \quad n \le N.$$

2.1. The first-order scheme. A first-order scheme for solving the system (2.2) can be readily derived by the backward Euler method. The first-order scheme can be written as follows:

$$\begin{cases} \dfrac{\phi^{n+1}-\phi^n}{\Delta t} = \mathcal{G}\mu^{n+1}, \\ \mu^{n+1} = \mathcal{L}\phi^{n+1} + b^{r^n,\phi^n}, \\ \dfrac{\ln(r^{n+1}) - \ln(r^n)}{\Delta t} = \left(b^{r^n,\phi^n}, \dfrac{\phi^{n+1}-\phi^n}{\Delta t}\right). \end{cases} \tag{2.7}$$

Multiplying the first two equations in (2.7) with μ^{n+1} and $(\phi^{n+1}-\phi^n)/\Delta t$, combining them with the third equation in (2.7), and noting the equation

$$(a-b,a) = \frac{1}{2}|a|^2 - \frac{1}{2}|b|^2 + \frac{1}{2}|a-b|^2,$$

we obtain the discrete energy law

$$\frac{1}{\Delta t}\left[E_{1st}^{n+1} - E_{1st}^n\right] \le (\mathcal{G}\mu^{n+1},\mu^{n+1}) - \frac{1}{2\Delta t}(\phi^{n+1}-\phi^n, \mathcal{L}(\phi^{n+1}-\phi^n)) \le 0, \tag{2.8}$$

where the modified discrete version of the energy is defined by

$$E_{1st}^n = \frac{1}{2}(\phi^n,\mathcal{L}\phi^n) + \ln(r^n).$$

Remark 2.2. The first-order E-SAV scheme (2.7) is much easier to implement than the traditional SAV, because the totally explicit computing of ϕ^{n+1} can be achieved. Furthermore, the implicit processing of r^{n+1} ensures the energy stability of the discrete

format. For the SAV scheme, which can be seen in [25], we have to compute the inner product (b^n, ϕ^{n+1}) before obtaining ϕ^{n+1}, where $b^n = F'(\phi^n)/\sqrt{E_1(\phi^n)}$. However, for the E-SAV scheme, we do not need to do this. We can compute ϕ^{n+1} directly by the first two equations in (2.7); then r^{n+1} can be very easy to obtain by computing $\left(b^{r^n,\phi^n}, \phi^{n+1} - \phi^n\right)$. That is to say, the computations of ϕ and r are totally decoupled. Thus, compared with the traditional SAV algorithm, the E-SAV algorithm greatly simplifies the calculation which is conducive to rapid simulation.

In particular, the first two equations in (2.7) can be written as

$$(I - \Delta t\mathcal{G}\mathcal{L})\phi^{n+1} = \phi^n + \Delta t\mathcal{G}b^{r^n,\phi^n}. \tag{2.9}$$

Multiplying (2.9) with $(I - \Delta t\mathcal{G}\mathcal{L})^{-1}$, we can obtain ϕ^{n+1} directly:

$$\phi^{n+1} = (I - \Delta t\mathcal{G}\mathcal{L})^{-1}\phi^n + \Delta t(I - \Delta t\mathcal{G}\mathcal{L})^{-1}\mathcal{G}b^{r^n,\phi^n}. \tag{2.10}$$

Substituting (2.10) into the third equation in (2.9), we can compute r^{n+1}:

$$r^{n+1} = \exp\left[\ln(r^n) + \left(b^{r^n,\phi^n}, \phi^{n+1} - \phi^n\right)\right]. \tag{2.11}$$

Remark 2.3. The logarithmic function in (2.6) guarantees the positive property of the auxiliary variable r. Meanwhile, for the discrete scheme, the exponential function in (2.11) guarantees the constant positive property of r^{n+1}, which makes $\ln(r^{n+1})$ reasonable to obtain r^{n+2}.

To summarize, we implement (2.7) as follows:
1. Compute r^n and ϕ^n.
2. Compute b^{r^n,ϕ^n} from $b^{r^n,\phi^n} = \frac{r^n}{\exp(E_1(\phi^n))}F'(\phi^n)$.
3. Compute ϕ^{n+1} from (2.10).
4. Compute r^{n+1} from (2.11).

2.2. The second-order scheme. A linear, second-order, sequentially solved and unconditionally stable E-SAV scheme is also very easy to construct. A semi-implicit E-SAV scheme based on the second-order Crank–Nicolson formula (CN) for (2.3) reads as follows: for $n \geq 1$,

$$\begin{cases} \dfrac{\phi^{n+1} - \phi^n}{\Delta t} = \mathcal{G}\mu^{n+\frac{1}{2}}, \\ \mu^{n+\frac{1}{2}} = \mathcal{L}\dfrac{\phi^{n+1} + \phi^n}{2} + b^{\tilde{r}^{n+\frac{1}{2}},\tilde{\phi}^{n+\frac{1}{2}}}, \\ \dfrac{\ln(r^{n+1}) - \ln(r^n)}{\Delta t} = \left(b^{\tilde{r}^{n+\frac{1}{2}},\tilde{\phi}^{n+\frac{1}{2}}}, \dfrac{\phi^{n+1} - \phi^n}{\Delta t}\right), \end{cases} \tag{2.12}$$

where $\tilde{\phi}^{n+\frac{1}{2}}$ is any explicit $O(\Delta t^2)$ approximation for $\phi(t^{n+\frac{1}{2}})$, and $\tilde{r}^{n+\frac{1}{2}}$ is any explicit $O(\Delta t^2)$ approximation for $r(t^{n+\frac{1}{2}})$, which can be flexible according to the problem. Here, we choose

$$\begin{aligned} \tilde{\phi}^{n+\frac{1}{2}} &= \frac{3}{2}\phi^n - \frac{1}{2}\phi^{n-1}, \quad n \geq 1, \\ \tilde{r}^{n+\frac{1}{2}} &= \frac{3}{2}r^n - \frac{1}{2}r^{n-1}, \quad n \geq 1, \end{aligned} \tag{2.13}$$

and for $n = 0$, we compute $\widetilde{\phi}^{\frac{1}{2}}$ as follows:

$$\frac{\widetilde{\phi}^{\frac{1}{2}} - \phi^0}{(\Delta t)/2} = \mathcal{G}\left[\mathcal{L}\widetilde{\phi}^{\frac{1}{2}} + F'(\phi^0)\right], \tag{2.14}$$

which has a local truncation error of $O(\Delta t^2)$.

Then we can compute $\widetilde{r}^{\frac{1}{2}}$ from

$$\widetilde{r}^{\frac{1}{2}} = \exp\left[\int_\Omega F(\widetilde{\phi}^{\frac{1}{2}})d\mathbf{x}\right]. \tag{2.15}$$

Similarly, ϕ^{n+1} can be solved by the following:

$$\phi^{n+1} = \left(I - \frac{1}{2}\Delta t\mathcal{G}\mathcal{L}\right)^{-1}\phi^n + \frac{1}{2}\left(I - \frac{1}{2}\Delta t\mathcal{G}\mathcal{L}\right)^{-1}\mathcal{G}\mathcal{L}\phi^n + \Delta t(I - \Delta t\mathcal{G}\mathcal{L})^{-1}\mathcal{G}b^{\widetilde{r}^{n+\frac{1}{2}},\widetilde{\phi}^{n+\frac{1}{2}}}. \tag{2.16}$$

Then we can compute r^{n+1} by ϕ^{n+1}:

$$r^{n+1} = \exp\left[\ln(r^n) + \left(b^{\widetilde{r}^{n+\frac{1}{2}},\widetilde{\phi}^{n+\frac{1}{2}}}, \phi^{n+1} - \phi^n\right)\right]. \tag{2.17}$$

Multiplying the first two equations in (2.12) with $\mu^{n+\frac{1}{2}}$ and $(\phi^{n+1} - \phi^n)/\Delta t$, and combining them with the third equation in (2.12), we derive the following.

THEOREM 2.1. *The scheme* (2.12) *for the equivalent phase field system* (2.3) *is second-order accurate and unconditionally energy stable in the sense that*

$$\frac{1}{\Delta t}\left[E^{n+1}_{E-SAV-CN} - E^n_{E-SAV-CN}\right] \le (\mathcal{G}\mu^{n+\frac{1}{2}}, \mu^{n+\frac{1}{2}}) \le 0,$$

where the modified discrete version of the energy is defined by

$$E^n_{E-SAV-CN} = \frac{1}{2}(\phi^n, \mathcal{L}\phi^n) + \ln(r^n).$$

Remark 2.4. The second-order E-SAV scheme (2.12) based on Crank–Nicolson can be implemented step by step as follows: (i) Compute the initial values of ϕ^0 and r^0. (ii) Compute $\tilde{\phi}^{\frac{1}{2}}$ from (2.14) and $\tilde{r}^{\frac{1}{2}}$ from (2.15). (iii) Compute ϕ^1 from (2.16). (iv) Compute r^1 from (2.17). (v) Compute ϕ^n from (2.16) for $n \ge 2$. (vi) Compute r^n from (2.17) for $n \ge 2$.

Remark 2.5. As for the error estimate for the E-SAV approach, we can follow the main process in [23] by deriving the H^2 bound for the phase function first. Since the main contribution of our work is the construction of the optimal technique of the SAV approach, we will consider this work in the future.

3. E-SAV approach for phase field models of several functions. In this section, we consider the E-SAV approach for phase field models of multiple functions $\phi_1, \phi_2, \ldots, \phi_k$ $(k \ge 2)$. The energy functional will be [25]

$$E(\phi_1, \phi_2, \ldots, \phi_k) = \sum_{i,j=1}^{k} d_{i,j}(\mathcal{L}\phi_i, \phi_j) + \sum_{j=1}^{k}\int_\Omega F(\phi_j)d\mathbf{x}, \tag{3.1}$$

where $\mathcal{L}$ is a self-adjoint nonnegative linear operator, and the constant matrix $A = (d_{i,j})$ is symmetric positive definite.

Some applications involve coupled linear operators which render the phase field models of several functions very difficult to solve numerically using existing methods. By introducing an SAV approach can solve this problem very efficiently. In this

section, we try to use an E-SAV approach to obtain a more efficient and simpler algorithm to solve phase field models of multiple functions.

We set $E_1(\phi) = \sum_{j=1}^{k} \int_\Omega F(\phi_j) d\mathbf{x}$, then introduce an exponential scalar auxiliary variable:

$$r(t) = \exp\left(E_1(\phi_1, \phi_2, \ldots, \phi_k)\right) = \exp\left(\sum_{j=1}^{k} \int_\Omega F(\phi_j) d\mathbf{x}\right). \tag{3.2}$$

Then we can obtain the phase field models from the energetic variation of the energy functional $E(\phi)$ in (3.1) as follows:

$$\begin{cases} \dfrac{\partial \phi_i}{\partial t} = \mathcal{G}\mu_i, \\ \mu_i = 2\displaystyle\sum_{j=1}^{k} d_{i,j}\mathcal{L}\phi_j + \dfrac{r}{\exp\left(E_1(\phi_1, \phi_2, \ldots, \phi_k)\right)} F_i', \\ \dfrac{d \ln r}{dt} = \dfrac{r}{\exp\left(E_1(\phi_1, \phi_2, \ldots, \phi_k)\right)} \displaystyle\int_\Omega F'(\phi_i) \frac{\partial \phi_i}{\partial t} d\mathbf{x}. \end{cases} \tag{3.3}$$

To simplify the notation, we define

$$b^{r,\phi_i} = \frac{r}{\exp\left(E_1(\phi_1, \phi_2, \ldots, \phi_k)\right)} F_i'.$$

Then the above system (3.3) can be transformed as follows:

$$\begin{cases} \dfrac{\partial \phi_i}{\partial t} = \mathcal{G}\mu_i, \\ \mu_i = 2\displaystyle\sum_{j=1}^{k} d_{i,j}\mathcal{L}\phi_j + b^{r,\phi_i}, \\ \dfrac{d \ln r}{dt} = \left(b^{r,\phi_i}, \dfrac{\partial \phi_i}{\partial t}\right). \end{cases} \tag{3.4}$$

Taking the inner products of the first two equations with μ_i and $\frac{d\phi_i}{dt}$ in (3.4), respectively, combining them with the third equation in (3.4), and summing over i, we obtain that

$$\frac{d}{dt}\left[\sum_{i,j=1}^{k} d_{i,j}(\mathcal{L}\phi_i, \phi_j) + \ln r\right] = \frac{d}{dt} E(\phi_1, \phi_2, \ldots, \phi_k) = \sum_{i=1}^{k} (\mathcal{G}\mu_i, \mu_i) \le 0.$$

A linear, second-order, sequentially solved and unconditionally stable E-SAV scheme based on the Crank–Nicolson formula can be constructed as follows:

$$\begin{cases} \dfrac{\phi_i^{n+1} - \phi_i^n}{\Delta t} = \mathcal{G}\mu_i^{n+\frac{1}{2}}, \\ \mu_i^{n+\frac{1}{2}} = \displaystyle\sum_{j=1}^{k} d_{i,j}\mathcal{L}(\phi_j^{n+1} + \phi_j^n) + b^{\tilde{r}^{n+\frac{1}{2}}, \tilde{\phi}_i^{n+\frac{1}{2}}}, \\ \dfrac{\ln(r^{n+1}) - \ln(r^n)}{\Delta t} = \left(b^{\tilde{r}^{n+\frac{1}{2}}, \tilde{\phi}_i^{n+\frac{1}{2}}}, \dfrac{\phi_i^{n+1} - \phi_i^n}{\Delta t}\right), \end{cases} \tag{3.5}$$

where $\tilde{\phi}_i^{n+\frac{1}{2}}$ is any explicit $O(\Delta t^2)$ approximation for $\phi_i(t^{n+\frac{1}{2}})$, and $\tilde{r}^{n+\frac{1}{2}}$ is any explicit $O(\Delta t^2)$ approximation for $r(t^{n+\frac{1}{2}})$, which can be flexible according to the problem.

Multiplying the first two equations in (3.5) with $\mu_i^{n+\frac{1}{2}}$ and $(\phi_i^{n+1}-\phi_i^n)/\Delta t$, and combining them with the third equation in (3.5) and summing over i, we derive the following discrete energy law:

$$\frac{1}{\Delta t}\left[\sum_{i,j=1}^{k} d_{i,j}(\mathcal{L}\phi_i^{n+1},\phi_j^{n+1})+\ln(r^{n+1})-\sum_{i,j=1}^{k} d_{i,j}(\mathcal{L}\phi_i^{n},\phi_j^{n})-\ln(r^{n})\right]$$
$$=\sum_{i=1}^{k}(\mathcal{G}\mu_i^{n+\frac{1}{2}},\mu_i^{n+\frac{1}{2}})\le 0.$$

Next, we describe how the scheme (3.5) can be efficiently implemented. Denote

$$\Phi^n=(\phi_1^n,\phi_2^n,\dots,\phi_k^n),\quad B^n=(b^{\tilde{r}^{n+\frac{1}{2}},\tilde{\phi}_1^{n+\frac{1}{2}}},b^{\tilde{r}^{n+\frac{1}{2}},\tilde{\phi}_2^{n+\frac{1}{2}}},\dots,b^{\tilde{r}^{n+\frac{1}{2}},\tilde{\phi}_k^{n+\frac{1}{2}}}). \tag{3.6}$$

Then,Φ^{n+1} can be computed by the following equation:

$$\Phi^{n+1}=(I-\Delta t\mathcal{G}A\mathcal{L})^{-1}\Phi^n+\frac{1}{2}(I-\Delta t\mathcal{G}A\mathcal{L})^{-1}\mathcal{G}A\mathcal{L}\Phi^n+\Delta t(I-\Delta t\mathcal{G}A\mathcal{L})^{-1}\mathcal{G}B^n. \tag{3.7}$$

Then we can compute r^{n+1} by any ϕ_i^{n+1}:

$$r^{n+1}=\exp\left[\ln(r^n)+\left(b^{\tilde{r}^{n+\frac{1}{2}},\tilde{\phi}_i^{n+\frac{1}{2}}},\phi_i^{n+1}-\phi_i^n\right)\right]. \tag{3.8}$$

Remark 3.1. The second-order E-SAV scheme (3.5) based on Crank–Nicolson can be implemented step by step as follows: (i) Compute the initial values of ϕ_i^0 for $i=1,\dots,k$ and r^0. (ii) Compute $\tilde{\phi}_i^{\frac{1}{2}}$ for $i=1,\dots,k$ and $\tilde{r}^{\frac{1}{2}}$. (iii) Compute Φ^1 from (3.7). (iv) Compute r^1 from (3.8). (v) Compute Φ^n from (3.7) for $n\ge 2$. (iv) Compute r^n from (3.8) for $n\ge 2$.

From the above remark, it is not difficult to find that Φ^{n+1} and r^{n+1} can be computed step by step. We do not need to compute the inner products $(b^{\tilde{r}^{n+\frac{1}{2}},\tilde{\phi}_i^{n+\frac{1}{2}}},\phi_i^{n+1})$ for $i=1,\dots,k$, such as in the traditional SAV scheme, before obtaining Φ^{n+1}, which can simplify the calculation greatly.

4. Modified E-SAV approach. In calculation, we notice that the exponential function is a rapidly increasing function which carries the risk of failure for the E-SAV approach. In this section, by adding a positive constant C in the exponential scalar auxiliary variable, we can improve it greatly. In particular, define a new exponential scalar auxiliary variable:

$$r(t)=\exp\left(\frac{E_1(\phi)}{C}\right)=\exp\left(\frac{1}{C}\int_\Omega F(\phi)d\mathbf{x}\right). \tag{4.1}$$

Then the phase field system (2.2) can be transformed as follows:

$$\begin{cases}\dfrac{\partial\phi}{\partial t}=\mathcal{G}\mu,\\ \mu=\mathcal{L}\phi+b^{r,\phi},\\ \dfrac{d\ln r}{dt}=\dfrac{1}{C}(b^{r,\phi},\phi_t),\end{cases} \tag{4.2}$$

where we set $b^{r,\phi} = [rF'(\phi)]/\exp(E_1(\phi)/C)$.

Taking the inner products of the first two equations above with μ, ϕ_t, respectively, and combining them with the third equation, we obtain that the above equivalent system satisfies the following energy dissipation law:

$$\frac{d}{dt}\left[\frac{1}{2}(\phi, \mathcal{L}\phi) + C\ln r\right] = (\mathcal{G}\mu, \mu) \le 0.$$

Remark 4.1. Noting the definition of the auxiliary variable r, it is not difficult to obtain

$$\begin{aligned}\frac{d}{dt}\left[\frac{1}{2}(\phi, \mathcal{L}\phi) + C\ln r\right] &= \frac{d}{dt}\left[\frac{1}{2}(\phi, \mathcal{L}\phi) + C\ln\exp(E_1/C)\right] \\ &= \frac{d}{dt}\left[\frac{1}{2}(\phi, \mathcal{L}\phi) + E_1\right] = \frac{dE}{dt} = (\mathcal{G}\mu, \mu) \le 0,\end{aligned}$$

which means the above energy inequality is still totally equal to the original energy dissipation law for any fixed constant C.

Similar first-order and second-order discrete schemes can be obtained immediately. For example, the first-order E-SAV scheme can be written

$$\begin{cases} \dfrac{\phi^{n+1}-\phi^n}{\Delta t} = \mathcal{G}\mu^{n+1}, \\ \mu^{n+1} = \mathcal{L}\phi^{n+1} + b^{r^n,\phi^n}, \\ \dfrac{\ln(r^{n+1}) - \ln(r^n)}{\Delta t} = \dfrac{1}{C}\left(b^{r^n,\phi^n}, \dfrac{\phi^{n+1}-\phi^n}{\Delta t}\right). \end{cases} \tag{4.3}$$

Obviously, we can choose C to be a big positive fixed constant. For the general phase field models, we can give some specific values. As we all know, the dissipative energy law means $\frac{d}{dt}E(\phi) \le 0$. Then an obvious property will hold as follows:

$$E(\phi(\mathbf{x},0)) \ge E(\phi(\mathbf{x},t)) \quad \forall \mathbf{x} \in \Omega, t \ge 0. \tag{4.4}$$

Considering the definition of the energy and noting that $\mathcal{L}$ is a symmetric nonnegative linear operator, it is not difficult to obtain the following inequality:

(4.5)

$$E(\phi(\mathbf{x},0)) - E_1(\phi(\mathbf{x},t)) = E(\phi(\mathbf{x},0)) - E(\phi(\mathbf{x},t)) + (\phi, \mathcal{L}\phi) \ge (\phi, \mathcal{L}\phi) \ge 0 \quad \forall \mathbf{x} \in \Omega, t \ge 0.$$

Hence, in practice calculation, we can choose $C = |E_1(\phi(\mathbf{x},0))|$ or $C = |E(\phi(\mathbf{x},0))|$.

5. Multiple E-SAV approach. Many complex phase field models include two or more unknown variables and nonlinear terms. A single scalar auxiliary variable cannot adequately describe the two or more evolution processes. In [8], the authors consider the multiple SAV approach for the phase field vesicle membrane model. To enhance the applicability of the proposed E-SAV approach, we construct the multiple E-SAV (ME-SAV) approach in this section in a general setting.

Mathematically, the complex phase field model is derived from the functional variation of free energy. In general, the free energy $E(\phi)$ contains the sum of an integral phase of some nonlinear functionals and a quadratic term:

$$E(\phi) = \frac{1}{2}(\phi, \mathcal{L}\phi) + \int_\Omega \sum_{i=1}^{k} F_i(\phi) d\mathbf{x},$$

where $\mathcal{L}$ is a symmetric nonnegative linear operator. Denote the chemical potential $\mu = \frac{\delta E}{\delta \phi}$. Then the phase field models from the energetic variation of the energy functional $E(\phi)$ can be obtained as follows:

$$\begin{cases} \dfrac{\partial \phi}{\partial t} = \mathcal{G}\mu, \\ \mu = \mathcal{L}\phi + \displaystyle\sum_{i=1}^{k} F_i'(\phi). \end{cases} \tag{5.1}$$

Introduce the following exponential scalar auxiliary variables:

$$r_i(t) = \exp\left(\frac{1}{C}\int_\Omega F_i(\phi) d\mathbf{x}\right), \tag{5.2}$$

where C is a big constant to make $r_i(t)$ a not very big number for every t. Similarly as before, an equivalent system of (5.1) can be written as follows:

$$\begin{cases} \dfrac{\partial \phi}{\partial t} = \mathcal{G}\mu, \\ \mu = \mathcal{L}\phi + \displaystyle\sum_{i=1}^{k} b_i^{r_i,\phi}, \\ \dfrac{d \ln r_i}{dt} = \dfrac{1}{C}\left(b_i^{r_i,\phi}, \dfrac{\partial \phi}{\partial t}\right), \\ b_i^{r_i,\phi} = \dfrac{r_i(t)}{\exp(\frac{1}{C}\int_\Omega F_i(\phi) d\mathbf{x})} F_i'(\phi). \end{cases} \tag{5.3}$$

Taking the inner products of the first two equations above with μ, ϕ_t, respectively, and summing up for i from 1 to k for the third equation, we obtain that the above equivalent system satisfies a modified energy dissipation law:

$$\frac{d}{dt}\left[\frac{1}{2}(\phi, \mathcal{L}\phi) + C\sum_{i=1}^{k} \ln r_i\right] = (\mathcal{G}\mu, \mu) \le 0.$$

The first-order scheme derived by the backward Euler method and the second-order scheme based on the Crank–Nicolson formula are very easy to obtain. In detail, the explicit first-order scheme is

$$\begin{cases} \dfrac{\phi^{n+1} - \phi^n}{\Delta t} = \mathcal{G}\mu^{n+1}, \\ \mu^{n+1} = \mathcal{L}\phi^{n+1} + \displaystyle\sum_{i=1}^{k} b_i^{r_i^n,\phi^n}, \\ \dfrac{\ln(r_i^{n+1}) - \ln(r_i^n)}{\Delta t} = \left(b_i^{r_i^n,\phi^n}, \dfrac{\phi^{n+1} - \phi^n}{\Delta t}\right), \\ b_i^{r_i^n,\phi^n} = \dfrac{r_i^n}{\exp(\frac{1}{C}\int_\Omega F_i(\phi^n) d\mathbf{x})} F_i'(\phi^n) \end{cases} \tag{5.4}$$

and the explicit second-order scheme is

$$\begin{cases} \dfrac{\phi^{n+1}-\phi^n}{\Delta t} = \mathcal{G}\mu^{n+1}, \\ \mu^{n+1} = \mathcal{L}\phi^{n+1} + \displaystyle\sum_{i=1}^{k} b_i^{\widetilde{r}_i^{n+\frac{1}{2}},\widetilde{\phi}^{n+\frac{1}{2}}}, \\ \dfrac{\ln(r_i^{n+1})-\ln(r_i^n)}{\Delta t} = \left(b_i^{\widetilde{r}_i^{n+\frac{1}{2}},\widetilde{\phi}^{n+\frac{1}{2}}}, \dfrac{\phi^{n+1}-\phi^n}{\Delta t} \right), \\ b_i^{r_i^{n+\frac{1}{2}},\widetilde{\phi}^{n+\frac{1}{2}}} = \dfrac{\widetilde{r}_i^{n+\frac{1}{2}}}{\exp(\frac{1}{C}\int_\Omega F_i(\widetilde{\phi}^{n+\frac{1}{2}})d\mathbf{x})} F_i'(\widetilde{\phi}^{n+\frac{1}{2}}), \end{cases} \tag{5.5}$$

where $\tilde{\phi}^{n+\frac{1}{2}}$ is any explicit $O(\Delta t^2)$ approximation for $\phi(t^{n+\frac{1}{2}})$, and $\tilde{r}_i^{n+\frac{1}{2}}$ is any explicit $O(\Delta t^2)$ approximation for $r_i(t^{n+\frac{1}{2}})$, which can be flexible according to the problem. Here, we choose

$$\begin{aligned} \tilde{\phi}^{n+\frac{1}{2}} &= \frac{3}{2}\phi^n - \frac{1}{2}\phi^{n-1}, \quad n \geq 1, \\ \tilde{r}_i^{n+\frac{1}{2}} &= \frac{3}{2}r_i^n - \frac{1}{2}r_i^{n-1}, \quad n \geq 1, \quad i = 1, 2, \ldots, k. \end{aligned} \tag{5.6}$$

It is not difficult to obtain the unconditional energy stability of the above two schemes.

THEOREM 5.1. *Scheme* (5.4) *for the equivalent phase field system* (5.3) *is linear, first-order accurate, unconditionally energy stable in the sense that*

$$\begin{aligned} &\frac{1}{\Delta t}\left[E_{ME-SAV-1st}^{n+1} - E_{ME-SAV-1st}^{n}\right] \\ &\leq (\mathcal{G}\mu^{n+\frac{1}{2}}, \mu^{n+\frac{1}{2}}) - \frac{1}{2\Delta t}(\phi^{n+1}-\phi^n, \mathcal{L}(\phi^{n+1}-\phi^n)) \leq 0, \end{aligned}$$

where the modified discrete version of the energy is defined by

$$E_{ME-SAV-1st}^{n} = \frac{1}{2}(\phi^n, \mathcal{L}\phi^n) + C\sum_{i=1}^{k}\ln(r_i^n),$$

and scheme (5.5) *for the equivalent phase field system* (5.3) *is linear, second-order accurate, unconditionally energy stable in the sense that*

$$\frac{1}{\Delta t}\left[E_{ME-SAV-CN}^{n+1} - E_{ME-SAV-CN}^{n}\right] \leq (\mathcal{G}\mu^{n+\frac{1}{2}}, \mu^{n+\frac{1}{2}}) \leq 0,$$

where the modified discrete version of the energy is defined by

$$E_{ME-SAV-CN}^{n} = \frac{1}{2}(\phi^n, \mathcal{L}\phi^n) + C\sum_{i=1}^{k}\ln(r_i^n).$$

5.1. ME-SAV approach for the Cahn–Hilliard phase field model of the binary fluid-surfactant system. In this section, we consider the proposed ME-SAV approach for the commonly used binary fluid-surfactant phase field model with

two coupled Cahn–Hilliard equations. In particular, the free energy of the system is given as follows:

(5.7)
$$E(\phi,\rho)=\int_\Omega\left(\frac{1}{2}|\nabla\phi|^2+\frac{\alpha}{2}(\Delta\phi)^2+\frac{1}{4\epsilon^2}F(\phi)+\frac{\beta}{2}|\nabla\rho|^2+\frac{1}{4\eta^2}G(\rho)-\theta\rho|\nabla\phi|^2\right)d\mathbf{x},$$

where the double-well Ginzburg–Landau potential $F(\phi)=(\phi^2-1)^2$ and $G(\rho)=\rho^2(\rho-\rho_s)^2$, where α, β, ϵ, ρ_s, and θ are all positive parameters.

Considering a gradient flow in H^{-1} which is derived from the functional variation of free energy (5.7) and introducing two chemical potentials ν_ϕ and μ_ρ, one can obtain the following Cahn–Hilliard phase field model of the binary fluid-surfactant system:

(5.8)
$$\begin{cases}\dfrac{\partial\phi}{\partial t}=M_\phi\Delta\mu_\phi,\\ \mu_\phi=-\Delta\phi+\alpha\Delta^2\phi+\dfrac{1}{\epsilon^2}F'(\phi)+2\theta\nabla\cdot(\rho\nabla\phi),\\ \dfrac{\partial\rho}{\partial t}=M_\rho\Delta\mu_\rho,\\ \mu_\rho=-\beta\Delta\rho+\dfrac{1}{\eta^2}G'(\rho)+\theta|\nabla\phi|^2.\end{cases}$$

The system satisfies an energy dissipation law:

$$\frac{d}{dt}E(\phi,\rho)=-M_\phi\|\nabla\mu_\phi\|^2-M_\rho\|\nabla\mu_\rho\|^2\le 0.$$

One can notice that the above coupled system has two nonlinear terms $F'(\phi)$ and $G'(\rho)$ which makes it very hard to handle with only one SAV. Thus, we introduce two exponential scalar auxiliary variables as follows:

(5.9)
$$\begin{aligned}r(t)&=\exp(E_F)=\exp\left(\int_\Omega F(\phi)d\mathbf{x}\right),\\ q(t)&=\exp(E_G)=\exp\left(\int_\Omega G(\rho)d\mathbf{x}\right).\end{aligned}$$

Combining equations (5.9) with the coupled system (5.8), and defining

$$\begin{aligned}b^{r,\phi}&=\frac{r(t)}{\exp(E_F)}F^{'}(\phi),\\ d^{q,\rho}&=\frac{q(t)}{\exp(E_G)}G^{'}(\rho),\end{aligned}$$

we can obtain the following equivalent PDE system as follows:

(5.10)
$$\begin{cases}\dfrac{\partial\phi}{\partial t}=M_\phi\Delta\mu_\phi,\\ \mu_\phi=-\Delta\phi+\alpha\Delta^2\phi+\dfrac{1}{\epsilon^2}b^{r,\phi}+2\theta\nabla\cdot(\rho\nabla\phi),\\ \dfrac{\partial\rho}{\partial t}=M_\rho\Delta\mu_\rho,\\ \mu_\rho=-\beta\Delta\rho+\dfrac{1}{\eta^2}d^{q,\rho}+\theta|\nabla\phi|^2,\\ \dfrac{d\ln r}{dt}=\left(b^{r,\phi},\dfrac{\partial\phi}{\partial t}\right),\\ \dfrac{d\ln q}{dt}=\left(d^{q,\rho},\dfrac{\partial\rho}{\partial t}\right).\end{cases}$$

The free energy (5.7) can be rewritten as

(5.11)
$$E(\phi,\rho,r,q)=\int_\Omega\left(\frac{1}{2}|\nabla\phi|^2+\frac{\alpha}{2}(\Delta\phi)^2+\frac{\beta}{2}|\nabla\rho|^2-\theta\rho|\nabla\phi|^2\right)d\mathbf{x}+\frac{1}{4\epsilon^2}\ln r+\frac{1}{4\eta^2}\ln q.$$

The phase field model is usually supplemented with the periodic boundary condition. So, for system (5.10), we assume that the density fields ϕ and ρ are periodic on Ω. The initial conditions read as

$$\phi|_{t=0}=\phi_0,\quad \rho_{t=0}=\rho_0,\quad r|_{t=0}=\exp(E_F(\phi_0)),\quad q|_{t=0}=\exp(E_G(\rho_0)). \tag{5.12}$$

Taking the L^2 inner product of the first four equations in (5.10) with μ_ϕ, ϕ_t, μ_ρ, and ρ_t, respectively, and combining them with the last two equations in (5.10), we can obtain the energy dissipation law immediately:

$$\frac{d}{dt}E(\phi,\rho,r,q)=-M_\phi\|\nabla\mu_\phi\|^2-M_\rho\|\nabla\mu_\rho\|^2\le 0.$$

Next, we will give a first-order ME-SAV scheme and prove the unconditional energy stability. The second-order scheme based on the ME-SAV approach can be obtained similarly as before. In detail, the first-order scheme can be written as follows:

$$\textbf{Step I:}\begin{cases}\dfrac{\rho^{n+1}-\rho^n}{\Delta t}=M_\rho\Delta\mu_\rho^{n+1},\\ \mu_\rho^{n+1}=-\beta\Delta\rho^{n+1}+\dfrac{1}{\eta^2}d^{q^n,\rho^n}+\theta|\nabla\phi^n|^2,\\ \dfrac{\ln q^{n+1}-\ln q^n}{\Delta t}=\left(d^{q^n,\rho^n},\dfrac{\rho^{n+1}-\rho^n}{\Delta t}\right).\end{cases} \tag{5.13}$$

$$\textbf{Step II:}\begin{cases}\dfrac{\phi^{n+1}-\phi^n}{\Delta t}=M_\phi\Delta\mu_\phi^{n+1},\\ \mu_\phi^{n+1}=-\Delta\phi^{n+1}+\alpha\Delta^2\phi^{n+1}+\dfrac{1}{\epsilon^2}b^{r^n,\phi^n}\\ \qquad\qquad+2\theta\nabla\cdot\left(\rho^{n+1}\nabla\frac{\phi^n+1+\phi^n}{2}\right),\\ \dfrac{\ln r^{n+1}-\ln r^n}{\Delta t}=\left(b^{r^n,\phi^n},\dfrac{\phi^{n+1}-\phi^n}{\Delta t}\right).\end{cases} \tag{5.14}$$

Remark 5.1. The computations of ϕ, ρ, r, and q are totally decoupled by the above two steps. First, we only need ϕ^n to compute ρ^{n+1} in Step I. Then q^{n+1} can be obtained by computing $(d^{q^n,\rho^n},\rho^{n+1}-\rho^n)$. Next, when computing ϕ^{n+1} in Step II, ρ^{n+1} has already been obtained from Step I. Last, r^{n+1} can be obtained by computing $(b^{r^n,\phi^n},\phi^{n+1}-\phi^n)$.

THEOREM 5.2. *The scheme* (5.13)–(5.14) *for the equivalent system* (5.10) *is unconditionally energy stable in the sense that*

$$\frac{1}{\Delta t}\left[E_{ME-SAV}^{n+1}-E_{ME-SAV}^{n}\right]\le -M_\phi\|\nabla\mu_\phi^{n+1}\|^2-M_\rho\|\nabla\mu_\rho^{n+1}\|^2\le 0,$$

where the modified discrete version of the energy is defined by

$$\begin{aligned}E_{ME-SAV}^n=&\frac{\beta}{2\Delta t}\|\nabla\rho^n\|^2+\frac{1}{\eta^2}\ln q^n+\frac{1}{2\Delta t}\|\nabla\phi^n\|^2+\frac{\alpha}{2\Delta t}\|\Delta\phi^n\|^2\\&+\frac{1}{\epsilon^2\Delta t}\ln r^n-\frac{\theta}{\Delta t}(|\nabla\phi^n|^2,\rho^n).\end{aligned}$$

Proof. By taking the L^2 inner product with μ_ρ^{n+1} of the first equation in (5.13), we obtain

$$\frac{1}{\Delta t}(\rho^{n+1}-\rho^n,\mu_\rho^{n+1}) = -M_\rho\|\nabla\mu_\rho^{n+1}\|^2. \tag{5.15}$$

By taking the L^2 inner product of the second equation in (5.13) with $\frac{1}{\Delta t}(\rho^{n+1}-\rho^n)$, noticing that

$$(x,x-y)=\frac{1}{2}|x|^2+\frac{1}{2}|y|^2+\frac{1}{2}|x-y|^2,$$

then combining them with the third equation in (5.13), we obtain

$$\begin{aligned}\frac{1}{\Delta t}(\rho^{n+1}-\rho^n,\mu_\rho^{n+1}) &= \frac{\beta}{2\Delta t}(\|\nabla\rho^{n+1}\|^2-\|\nabla\rho^n\|^2+\|\nabla\rho^{n+1}-\nabla\rho^n\|^2)\\ &\quad+\frac{1}{\eta^2\Delta t}(\ln q^{n+1}-\ln q^n)\\ &\quad+\frac{\theta}{\Delta t}(|\nabla\phi^n|^2,\rho^{n+1}-\rho^n).\end{aligned} \tag{5.16}$$

By taking the L^2 inner product with μ_ϕ^{n+1} of the first equation in (5.14), we obtain

$$\frac{1}{\Delta t}(\phi^{n+1}-\phi^n,\mu_\phi^{n+1}) = -M_\phi\|\nabla\mu_\phi^{n+1}\|^2. \tag{5.17}$$

By taking the L^2 inner product of the second equation in (5.14) with $\frac{1}{\Delta t}(\phi^{n+1}-\phi^n)$, and combining them with the third equation in (5.14), we obtain

$$\begin{aligned}\frac{1}{\Delta t}(\phi^{n+1}-\phi^n,\mu_\phi^{n+1}) &= \frac{1}{2\Delta t}(\|\nabla\phi^{n+1}\|^2-\|\nabla\phi^n\|^2+\|\nabla\phi^{n+1}-\nabla\phi^n\|^2)\\ &\quad+\frac{\alpha}{2\Delta t}(\|\Delta\phi^{n+1}\|^2-\|\Delta\phi^n\|^2+\|\Delta\phi^{n+1}-\Delta\phi^n\|^2)\\ &\quad+\frac{1}{\epsilon^2\Delta t}(\ln r^{n+1}-\ln r^n)+\frac{\theta}{\Delta t}(|\nabla\phi^{n+1}|^2-|\nabla\phi^n|^2,\rho^{n+1}).\end{aligned} \tag{5.18}$$

Combining (5.15)–(5.18) and using the equality [36]

$$\begin{aligned}&\frac{\theta}{\Delta t}(|\nabla\phi^n|^2,\rho^{n+1}-\rho^n)+\frac{\theta}{\Delta t}(|\nabla\phi^{n+1}|^2-|\nabla\phi^n|^2,\rho^{n+1})\\ &=\frac{\theta}{\Delta t}(|\nabla\phi^{n+1}|^2,\rho^{n+1})-\frac{\theta}{\Delta t}(|\nabla\phi^n|^2,\rho^n),\end{aligned} \tag{5.19}$$

we have

$$\begin{aligned}&\frac{1}{\Delta t}\left[E_{ME-SAV}^{n+1}-E_{ME-SAV}^{n}\right]\\ &=\frac{\beta}{2\Delta t}\|\nabla\rho^{n+1}\|^2+\frac{1}{\eta^2}\ln q^{n+1}+\frac{1}{2\Delta t}\|\nabla\phi^{n+1}\|^2+\frac{\alpha}{2\Delta t}\|\Delta\phi^{n+1}\|^2\\ &\quad+\frac{1}{\epsilon^2\Delta t}\ln r^{n+1}-\frac{\theta}{\Delta t}(|\nabla\phi^{n+1}|^2,\rho^{n+1})\\ &\quad-\frac{\beta}{2\Delta t}\|\nabla\rho^n\|^2-\frac{1}{\eta^2}\ln q^n-\frac{1}{2\Delta t}\|\nabla\phi^n\|^2-\frac{\alpha}{2\Delta t}\|\Delta\phi^n\|^2-\frac{1}{\epsilon^2\Delta t}\ln r^n+\frac{\theta}{\Delta t}(|\nabla\phi^n|^2,\rho^n)\\ &=-M_\phi\|\nabla\mu_\phi^{n+1}\|^2-M_\rho\|\nabla\mu_\rho^{n+1}\|^2-\frac{\beta}{2\Delta t}\|\nabla\rho^{n+1}-\nabla\rho^n\|^2\\ &\quad-\frac{1}{2\Delta t}\|\nabla\phi^{n+1}-\nabla\phi^n\|^2-\frac{\alpha}{2\Delta t}\|\Delta\phi^{n+1}-\Delta\phi^n\|^2.\end{aligned} \tag{5.20}$$

∎

6. Examples and discussion. In this section, we use several numerical examples to demonstrate the accuracy, energy stability, and efficiency of the proposed schemes when applying them to some classical phase field models such as the Allen–Cahn equation, the Cahn–Hilliard equation, and the phase field crystal model. In all of the examples, we assume periodic boundary conditions and use a Fourier spectral method [7] for space variables. Some other methods, such as the finite difference method [29, 33] and the finite element method [13], can also be used to make the space variables discrete. To test the efficiency of fast calculation, all the solvers are implemented using MATLAB and all the numerical experiments are performed on a computer with 8GB memory.

6.1. Allen–Cahn and Cahn–Hilliard equations. Both the Allen–Cahn and Cahn–Hilliard equations are very classical phase field models and have been widely used in many fields involving physics, materials science, finance, and image processing [6, 10, 42]. In particular, the Allen–Cahn equation, introduced by M. Allen and W. Cahn in [1], has been widely used to model various phenomena in nature:

$$\begin{cases} \dfrac{\partial \phi}{\partial t} = -M\mu, & (\mathbf{x}, t) \in \Omega \times J, \\ \mu = -\Delta \phi + \dfrac{1}{\epsilon^2} f(\phi), & (\mathbf{x}, t) \in \Omega \times J; \end{cases} \tag{6.1}$$

the Cahn–Hilliard equation was introduced in [3] by John W. Cahn and John E. Hilliard to describe the process of phase separation,

$$\begin{cases} \dfrac{\partial \phi}{\partial t} = M\Delta \mu, & (\mathbf{x}, t) \in \Omega \times J, \\ \mu = -\epsilon \Delta \phi + \dfrac{1}{\epsilon} f(\phi), & (\mathbf{x}, t) \in \Omega \times J, \end{cases} \tag{6.2}$$

where $J = (0, T]$, M is the mobility constant, μ is the chemical potential, and $f(\phi) = F'(\phi)$, $F(\phi)$ is a nonconvex potential density function. In this paper, we consider the following double-well potential function $F(\phi) = \frac{1}{4}(\phi^2 - 1)^2$.

Example 1. Consider the above Allen–Cahn and Cahn–Hilliard equations in $\Omega = [0, 2\pi]$ with $\epsilon = 0.1$, $T = 0.032$, $M = 1$ in the Allen–Cahn equation and $M = 0.1$ in the Cahn–Hilliard equation, and the following initial condition [25]:

$$\phi(x, y, 0) = 0.05 \sin(x) \sin(y).$$

We use the Fourier spectral Galerkin method for spatial discretization with $N = 128$. The true solution is unknown, and we therefore use the Fourier–Galerkin approximation in the case $\Delta t =$ 1e-8 as a reference solution.

For the Allen–Cahn equation, we consider first-order time discrete schemes based on both the SAV approach in [25] and the proposed E-SAV approach in this article. The computational results are shown in Table 6.1. The numerical results indicate that both the SAV and E-SAV schemes are indeed of first order in time, but the later scheme keeps the error smaller. Specially, the E-SAV scheme is much easier to calculate than the SAV scheme. The CPU time shows that the E-SAV scheme is about half as time-consuming as the SAV scheme.

For the Cahn–Hilliard model, a comparative study of classical SAV and E-SAV approaches based on second-order time discrete schemes is considered in Table 6.2. The two methods obtain almost identical error and convergence rates. However, the E-SAV scheme also saves half the time compared with the SAV scheme.

TABLE 6.1
The L_2 errors and convergence rates for the first-order scheme in time for the SAV and E-SAV approaches of the Allen–Cahn equation.

	SAV			E-SAV		
Δt	L_2 error	Rate	CPU time(s)	L_2 error	Rate	CPU time(s)
1.6e-4	1.5839e-2	—	1.17	8.8644e-3	—	0.65
8e-5	7.9574e-3	0.9946	2.26	4.4254e-3	1.0022	1.29
4e-5	3.9680e-3	1.0052	4.51	2.1899e-3	1.0149	2.60
2e-5	1.9610e-3	1.0187	9.16	1.0681e-3	1.0358	4.78
1e-5	9.5446e-4	1.0422	17.83	5.0627e-4	1.0771	9.95

TABLE 6.2
The L_2 errors and convergence rates for second-order scheme in time for the SAV and E-SAV approaches of the Cahn–Hilliard equation.

	SAV			E-SAV		
Δt	L_2 error	Rate	CPU time(s)	L_2 error	Rate	CPU time(s)
1.6e-4	5.1526e-8	—	1.43	5.1474e-8	—	0.81
8e-5	1.2873e-8	2.0009	2.94	1.2848e-8	2.0023	1.43
4e-5	3.2156e-9	2.0011	5.07	3.2081e-9	2.0017	2.63
2e-5	8.0229e-10	2.0028	10.32	8.0147e-10	2.0009	5.63
1e-5	1.9906e-10	2.0109	20.12	1.9971e-10	2.0047	10.73

Example 2. In the following, we solve a benchmark problem for the Allen–Cahn equation which can be seen in many articles such as [25]. We take $\epsilon = 0.01$, $M = 1$. The initial condition is chosen as

$$\phi_0(x, y, 0) = \sum_{i=1}^{2} -\tanh\left(\frac{\sqrt{(x - x_i)^2 + (y - y_i)^2} - R_0}{\sqrt{2}\epsilon}\right) + 1,$$

with the radius $R_0 = 0.19$, $(x_1, y_1) = (0.3, 0.5)$, and $(x_2, y_2) = (0.7, 0.5)$. Initially, two bubbles, centered at $(0.3, 0.5)$ and $(0.7, 0.5)$, respectively, are osculating or "kissing."

As is known to all, the Allen–Cahn equation does not conserve mass. So, in Figure 6.1, we can see that as time evolves, the two bubbles coalesce into a single bubble, which shrinks and finally disappears. A correct simulation of this phenomenon shows the effectiveness of our E-SAV approach. In Figure 6.2, we plot the time evolution of the energy functional with the different time step sizes $\Delta t = 0.001$, 0.01, 0.1, 1, and 2 using the first-order scheme based on the E-SAV approach. All energy curves show the monotonic decays for all time steps, which confirms that the algorithm E-SAV is unconditionally energy stable. Time evolution of the total free energy based on the SAV and E-SAV approaches is computed by using the time step $\Delta t = 0.001$ in the left panel in Figure 6.2. These two energy curves are almost identical, and they both decay monotonically at all times.

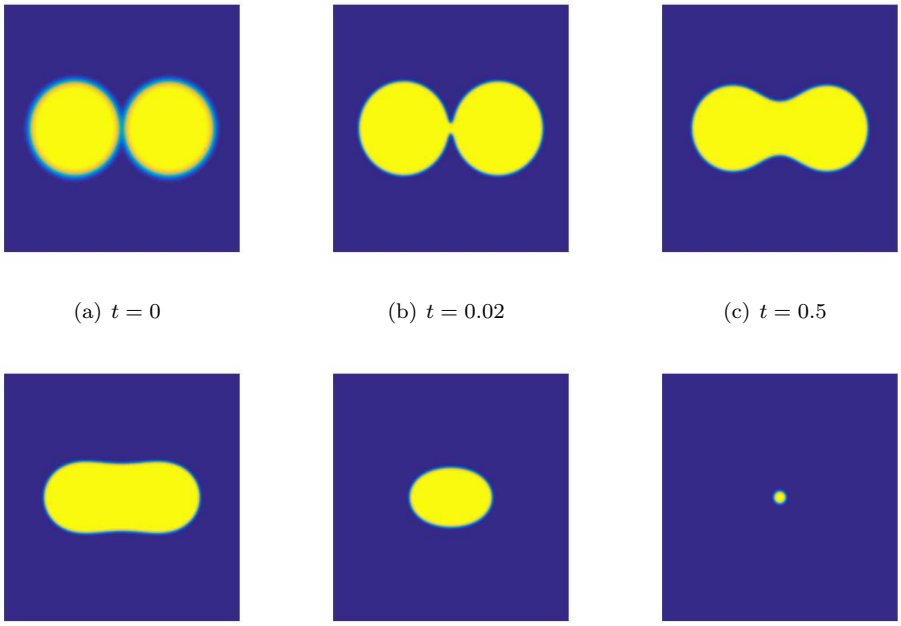

(a) $t = 0$ (b) $t = 0.02$ (c) $t = 0.5$

(d) $t = 1.5$ (e) $t = 4$ (f) $t = 5.6$

FIG. 6.1. *Snapshots of the phase variable ϕ are taken at $t = 0, 0.02, 0.5, 1.5, 4, 5.6$ for Example 2.*

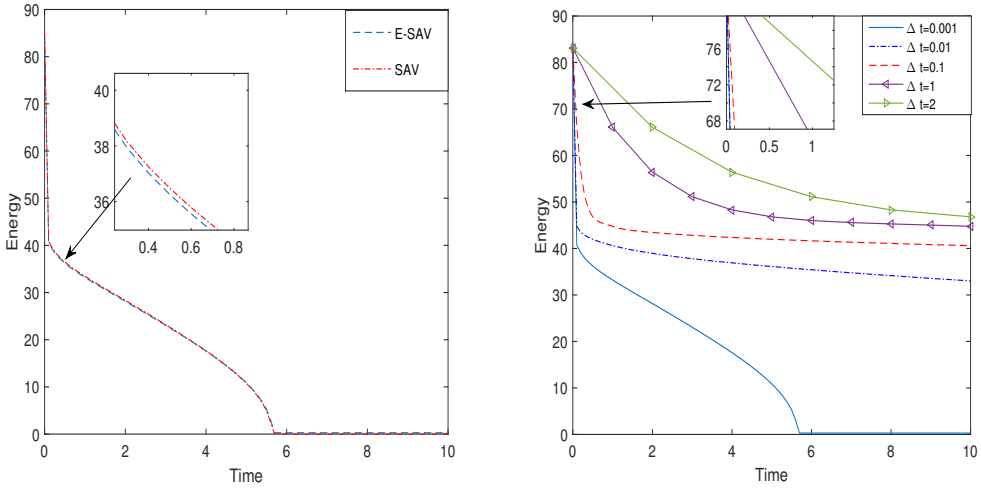

FIG. 6.2. *Left: energy evolution of the E-SAV and SAV approaches for Example 2 with $\Delta t = 0.001$. Right: time evolution of the energy functional for five different time steps, $\Delta t = 0.001$, 0.01, 0.1, 1, and 2.*

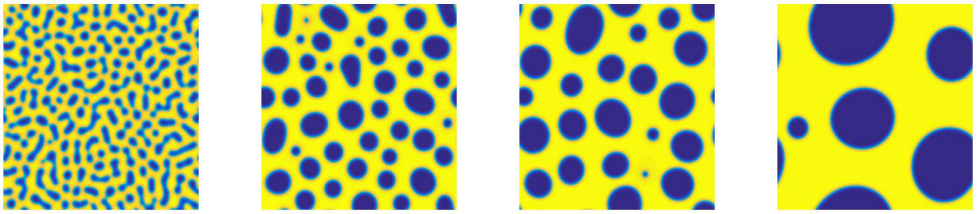

FIG. 6.3. *Snapshots of the phase variable ϕ are taken at $t = 0.02$, 0.5, 3, 20 for Example 3.*

Example 3. In the following, we solve a benchmark problem for the Cahn–Hilliard equation on $[0, 2\pi)^2$ which can also be seen in many articles such as [24]. We take $\epsilon = 0.02$, $M = 0.1$ and discretize the space by the Fourier spectral method with 256×256 modes. The initial condition is chosen as

$$\phi_0(x, y, 0) = 0.25 + 0.4\,\mathrm{Rand}(x, y),$$

where $\mathrm{Rand}(x, y)$ is a randomly generated function.

Snapshots of the phase variable ϕ taken at $t = 0.02$, 0.5, 3, and 20 with $\Delta t = 0.01$ are shown in Figure 6.3. The phase separation and coarsening process can be observed very simply, which is consistent with the results in [25].

6.2. Phase field crystal equations. A weakness of the traditional phase field methodology is that it is usually formulated in terms of fields that are spatially uniform in equilibrium. Elder et al. [11] first proposed the phase field crystal model based on density functional theory in 2002. This model can simulate the evolution of crystalline microstructures on atomistic length and diffusive time scales. It naturally incorporates elastic and plastic deformations and multiple crystal orientations and can be applied to many different physical phenomena.

In particular, consider the following Swift–Hohenberg free energy:

$$E(\phi) = \int_\Omega \left(\frac{1}{4}\phi^4 + \frac{1}{2}\phi \left(-\epsilon + (1 + \Delta)^2 \right) \phi \right) d\mathbf{x},$$

where $\mathbf{x} \in \Omega \subseteq \mathbb{R}^d$, ϕ is the density field, and ϵ is a positive bifurcation constant with physical significance. Δ is the Laplacian operator.

Considering a gradient flow in H^{-1}, one can obtain the phase field crystal equation under the constraint of mass conservation as follows:

$$\frac{\partial \phi}{\partial t} = \Delta \mu = \Delta \left(\phi^3 - \epsilon\phi + (1 + \Delta)^2 \phi \right), \quad (\mathbf{x}, t) \in \Omega \times Q,$$

which is a sixth-order nonlinear parabolic equation and can be applied to simulate various phenomena such as crystal growth, material hardness, and phase transition. Here $Q = (0, T]$, and $\mu = \frac{\delta E}{\delta \phi}$ is called the chemical potential.

Next, we plan to simulate the phase transition behavior of the phase field crystal model. Similar numerical examples can be found in many articles, such as [17, 37]. In Example 4 below, we study the crystal growth in a supercooled liquid in 2D. This example serves to show the applicability of our phase field crystal model to a physical problem [17].

Example 4. In the following, we take $\epsilon = 0.25$ to start our simulation on a domain $[0, 800] \times [0, 800]$ with a 512×512 mesh grid by Fourier spectral method in space and first-order E-SAV scheme in time. We generated the three crystallites using random perturbations on four small square paths. The following expression will be used to define the crystallites such as in [41]:

$$\phi(x_l, y_l) = \overline{\phi} + C\left(\cos\left(\frac{q}{\sqrt{3}}y_l\right)\cos(qx_l) - \frac{1}{2}\cos\left(\frac{2q}{\sqrt{3}}y_l\right)\right),$$

where x_l, y_l define a local system of Cartesian coordinates that is oriented with the crystallite lattice. We use the parameters $\overline{\phi} = 0.285$, $C = 0.446$, and $q = 0.66$. The local Cartesian system is defined as

$$x_l(x, y) = \mathrm{xsin}\,\theta + \mathrm{ycos}\,\theta,$$
$$y_l(x, y) = -\mathrm{xcos}\,\theta + \mathrm{ysin}\,\theta.$$

The centers of three paths are located at $(150, 150)$, $(200, 250)$, and $(250, 150)$ with $\theta = \pi/4$, 0, and $-\pi/4$. The length of each square is 40. Figure 6.4 shows the snapshots of the density field ϕ at different times. We observe the growth of the crystalline phase. We plot the energy dissipative curve in Figure 6.5 using three different time steps of $\delta t = 0.01$, 0.1, and 1. One can observe that the energy decreases at all times no matter whether the time steps are large or small. This expression of unconditional energy stability proved the efficiency of our proposed algorithm, as predicted by the former theory.

In Example 5 below, we check the difference of phase transition behavior between the proposed E-SAV method and the traditional SAV approach.

Example 5. The initial condition is

$$\phi_0(x, y) = 0.07 + 0.07\,\mathrm{Rand}(x, y),$$

where the $\mathrm{Rand}(x, y)$ is the random number in $[-1, 1]$ with zero mean. The order parameter is $\epsilon = 0.025$, and the computational domain is $\Omega = [0, 128]^2$. We set 256^2 Fourier modes to discretize the 2D space.

We show the phase transition behavior of the density field at various times in Figure 6.6. Similar computational results for the phase field crystal model can be found in [25, 37]. We investigate the process of crystallization in a supercooled liquid by using both the SAV and proposed E-SAV schemes. No visible difference is observed.

6.3. The Cahn–Hilliard phase field model of the binary fluid-surfactant system. In this subsection, we use several numerical examples to demonstrate the accuracy, energy stability, and efficiency of the proposed schemes based on the ME-SAV approach for the Cahn–Hilliard phase field model of the binary fluid-surfactant system. In the following two examples, we set the domain $\Omega = [0, 2\pi] \times [0, 2\pi]$. Other than that, the default values of parameters are given as follows:

$$M_\phi = M_\rho = 2.5e-4, \quad \alpha = 2.5e-4, \quad \beta = 1, \quad \theta = 0.3, \quad \epsilon = 0.05, \quad \eta = 0.08, \quad \rho_s = 1.$$

Example 6. We first test the error and the convergent rates of the proposed first-order ME-SAV scheme. The initial conditions are as follows:

$$\phi_0(x, y) = 0.3\mathrm{cos}(3x) + 0.5\mathrm{cos}(y),$$
$$\rho_0(x, y) = 0.2\mathrm{cos}(2x) + 0.25\mathrm{sin}(y).$$

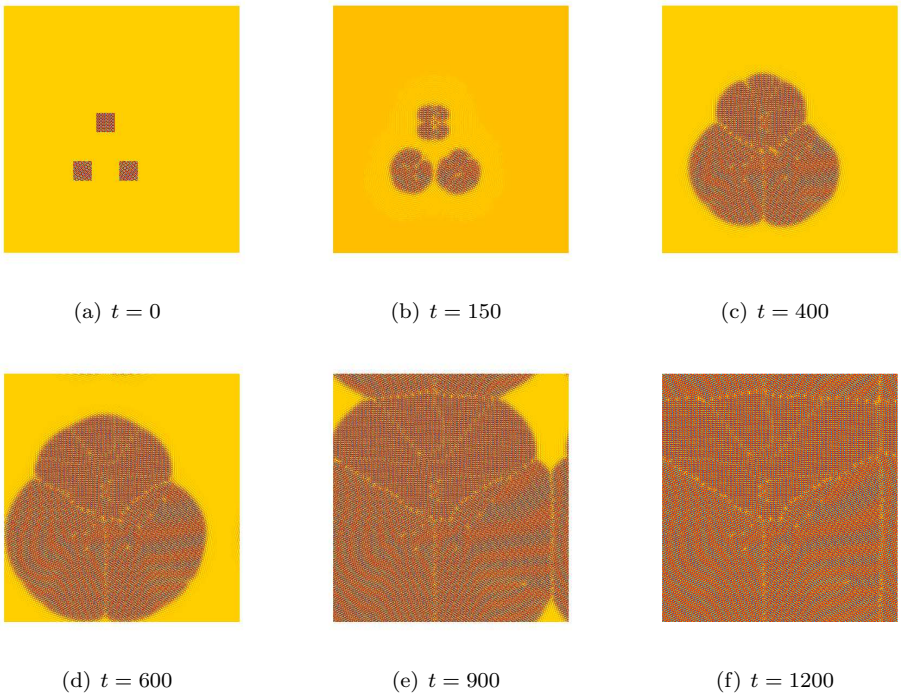

(a) $t = 0$ (b) $t = 150$ (c) $t = 400$

(d) $t = 600$ (e) $t = 900$ (f) $t = 1200$

FIG. 6.4. *Snapshots of the phase variable ϕ are taken at $t = 0, 150, 400, 600, 900, 1200$ for Example 4.*

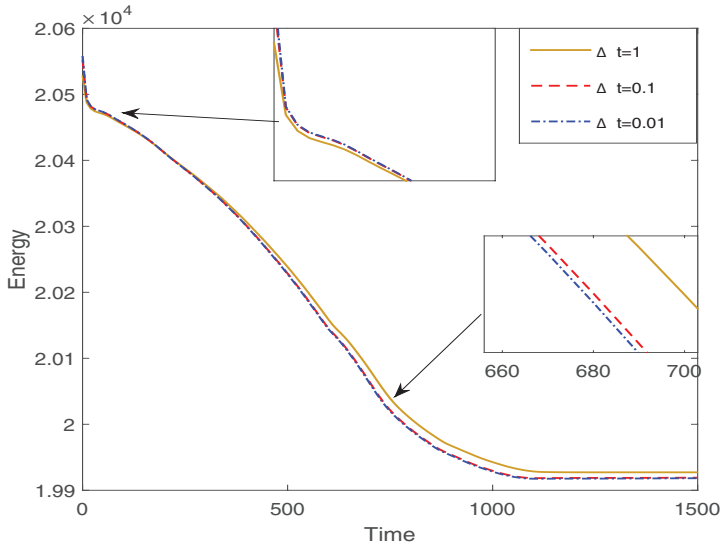

FIG. 6.5. *Energy evolution for the phase field crystal equation for Example 4 using E-SAV approaches with different time steps of $\delta t = 0.01$, 0.1, and 1.*

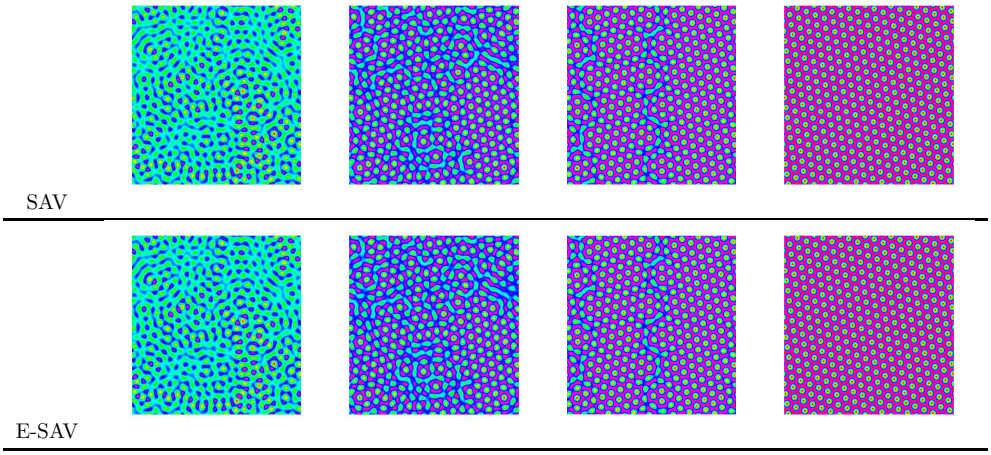

FIG. 6.6. *Configuration evolutions for the phase field crystal model by the SAV and E-SAV schemes are taken at* $t = 200$, 500, 1200, *and* 6000.

We use the Fourier spectral Galerkin method for spatial discretization with $N = 128$. The true solution is unknown, and we therefore use the Fourier–Galerkin approximation in the case $\Delta t =$ 1e-5 and $T = 0.1$ as a reference solution. Then we show the L^2 errors of two phase variables ϕ and ρ between the numerical solutions and the reference solutions with different time step sizes in Table 6.3. We observe that the convergence rates of both variables ϕ and ρ are all first-order accurate.

TABLE 6.3
The L_2 *errors and convergence rates for first-order scheme in time for the ME-SAV approach.*

		$\|\phi - \phi^n\|$		$\|\rho - \rho^n\|$	
	Δt	L_2 error	Rate	L_2 error	Rate
1st-ME-SAV	1e-2	2.5127e-3	—	1.0355e-4	—
	5e-3	1.3078e-3	0.9421	5.2007e-5	0.9935
	2.5e-3	6.6740e-4	0.9705	2.6019e-5	0.9991
	1.25e-3	3.3628e-4	0.9889	1.2972e-5	1.0041
	6.25e-4	1.6779e-4	1.0030	6.4364e-6	1.0111

In the next example, we study the phase separation behaviors, called spinodal decomposition, in the 2D space by using the first-order ME-SAV scheme.

Example 7. The initial conditions are taken as the following randomly perturbed concentration fields:

$$\phi_0(x, y) = 0.001\,\mathrm{Rand}(x, y),$$
$$\rho_0(x, y) = 0.2 + 0.001\,\mathrm{Rand}(x, y).$$

We set $\epsilon = 0.02$, $\eta = 0.005$. In Figure 6.7, we show the snapshots of two phase variables ϕ and ρ taken at $t = 1, 10, 20, 50, 100, 200, 400, 1000, 1500$, and 2000. One can see that the two fluids are well mixed at the beginning. As time goes on, because of the influence of the surface tensions, the two fluids start to decompose to equilibrium. However, a relatively high value of the concentration variable ρ is always driven to be located at the fluid interface. We also plot the evolution of energy curves in Figure 6.8 for Example 7 which indicates that the energy monotonically decays with respect to the time.

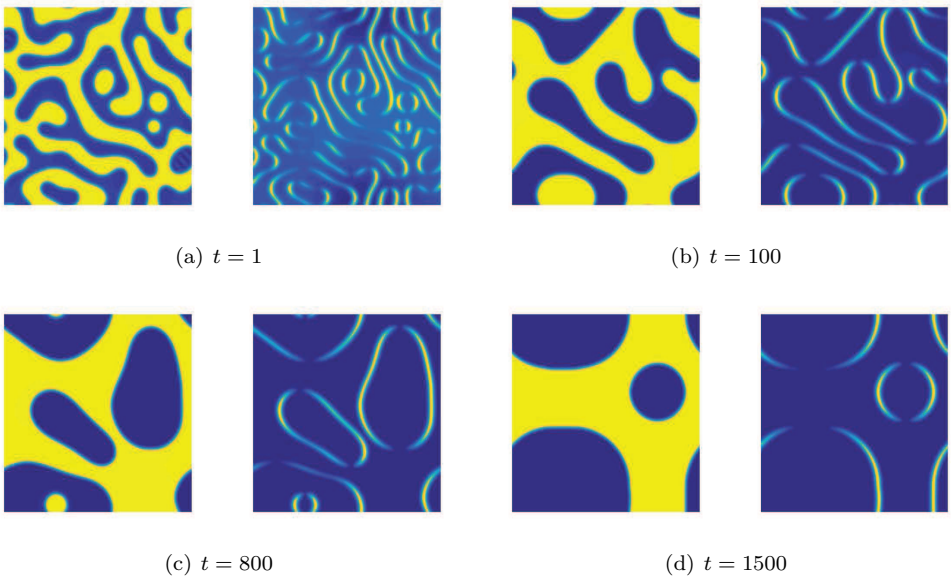

(a) $t = 1$ (b) $t = 100$

(c) $t = 800$ (d) $t = 1500$

FIG. 6.7. *Snapshots of the phase variable ϕ (left) and ρ (right) are taken at $t = 1, 100, 800, 1500$ for Example 7.*

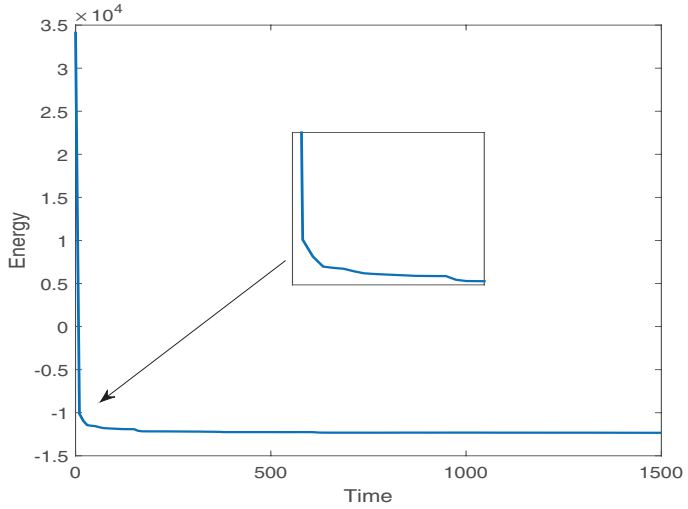

FIG. 6.8. *Time evolution of the free energy functional for spinodal decomposition.*

7. Concluding remarks. In this paper, an optimal technique for the popular SAV approach is proposed to obtain energy stable schemes for the phase field models. This novel method, called the E-SAV approach, has been proved more effective and applicable than the traditional SAV method to construct energy stable schemes. Details of this method follow:

(i) The auxiliary variable in the E-SAV approach is not based on any assumptions, while the nonlinear free energy potential has to be bounded from below in the SAV approach.

(ii) The positivity preserving property for r^n in the E-SAV approach is very important in obtaining the equivalent form of the original model. However, such a positive property of r^n cannot be guaranteed in the SAV approach.

(iii) The totally explicit energy stable schemes can be easily constructed by using our E-SAV approach, while such explicit schemes cannot preserve the energy dissipation law for the SAV approach.

(iv) The computations of ϕ^{n+1} and the auxiliary variable r^{n+1} can be solved step by step based on the E-SAV approach, while we have to compute an inner product before calculating ϕ^{n+1} in the SAV schemes.

(v) Schemes based on the E-SAV approach dissipate the original energy, as opposed to a modified energy in the SAV approach.

Furthermore, the numerical algorithm based on E-SAV approach can save much more computational time than that based on the SAV method. In addition, we consider a multiple E-SAV (ME-SAV) approach to enhance the applicability of the proposed E-SAV approach for complex phase field models with two or more unknown variables and nonlinear terms.

REFERENCES

[1] S. M. Allen and J. W. Cahn, *A microscopic theory for antiphase boundary motion and its application to antiphase domain coarsening*, Acta Metallurgica, 27 (1979), pp. 1085–1095.

[2] M. Ambati, T. Gerasimov, and L. De Lorenzis, *A review on phase-field models of brittle fracture and a new fast hybrid formulation*, Comput. Mech., 55 (2015), pp. 383–405.

[3] J. W. Cahn and J. E. Hilliard, *Free energy of a nonuniform system.* I. *Interfacial free energy*, J. Chem. Phys., 28 (1958), pp. 258–267.

[4] C. Chen and X. Yang, *Efficient numerical scheme for a dendritic solidification phase field model with melt convection*, J. Comput. Phys., 388 (2019), pp. 41–62.

[5] C. Chen and X. Yang, *Fast, provably unconditionally energy stable, and second-order accurate algorithms for the anisotropic Cahn-Hilliard model*, Comput. Methods Appl. Mech. Engrg., 351 (2019), pp. 35–59.

[6] L. Chen, J. Zhang, J. Zhao, W. Cao, H. Wang, and J. Zhang, *An accurate and efficient algorithm for the time-fractional molecular beam epitaxy model with slope selection*, Comput. Phys. Commun., 245 (2019), 106842.

[7] L. Q. Chen and J. Shen, *Applications of semi-implicit Fourier-spectral method to phase field equations*, Comput. Phys. Commun., 108 (1998), pp. 147–158.

[8] Q. Cheng and J. Shen, *Multiple scalar auxiliary variable (MSAV) approach and its application to the phase-field vesicle membrane model*, SIAM J. Sci. Comput., 40 (2018), pp. A3982–A4006, https://doi.org/10.1137/18M1166961.

[9] Q. Du, L. Ju, X. Li, and Z. Qiao, *Maximum principle preserving exponential time differencing schemes for the nonlocal Allen–Cahn equation*, SIAM J. Numer. Anal., 57 (2019), pp. 875–898, https://doi.org/10.1137/18M118236X.

[10] Q. Du, L. Ju, X. Li, and Z. Qiao, *Stabilized linear semi-implicit schemes for the nonlocal Cahn-Hilliard equation*, J. Comput. Phys., 363 (2018), pp. 39–54.

[11] K. Elder, M. Katakowski, M. Haataja, and M. Grant, *Modeling elasticity in crystal growth*, Phys. Rev. Lett., 88 (2002), 245701.

[12] D. J. Eyre, *Unconditionally gradient stable time marching the Cahn-Hilliard equation*, in Computational and Mathematical Models of Microstructural Evolution (San Francisco, CA, 1998), Mater. Res. Soc. Sympos. Proc. 529, MRS, Warrendale, PA, 1998, pp. 39–46.

[13] X. Feng, Y. He, and C. Liu, *Analysis of finite element approximations of a phase field model for two-phase fluids*, Math. Comp., 76 (2007), pp. 539–571.

[14] Z. Guo and P. Lin, *A thermodynamically consistent phase-field model for two-phase flows with thermocapillary effects*, J. Fluid Mech., 766 (2015), pp. 226–271.

[15] D. Hou, M. Azaiez, and C. Xu, *A variant of scalar auxiliary variable approaches for gradient flows*, J. Comput. Phys., 395 (2019), pp. 307–332.

[16] X. Li, J. Shen, and H. Rui, *Energy stability and convergence of SAV block-centered finite difference method for gradient flows*, Math. Comp., 88 (2019), pp. 2047–2068.

[17] Y. Li and J. Kim, *An efficient and stable compact fourth-order finite difference scheme for the*

phase field crystal equation, Comput. Methods Appl. Mech. Engrg., 319 (2017), pp. 194–216.

[18] L. Lin, Z. Yang, and S. Dong, *Numerical approximation of incompressible Navier-Stokes equations based on an auxiliary energy variable*, J. Comput. Phys., 388 (2019), pp. 1–22.

[19] Z. Liu and X. Li, *Efficient modified techniques of invariant energy quadratization approach for gradient flows*, Appl. Math. Lett., 98 (2019), pp. 206–214.

[20] W. Marth, S. Aland, and A. Voigt, *Margination of white blood cells: A computational approach by a hydrodynamic phase field model*, J. Fluid Mech., 790 (2016), pp. 389–406.

[21] C. Miehe, M. Hofacker, and F. Welschinger, *A phase field model for rate-independent crack propagation: Robust algorithmic implementation based on operator splits*, Comput. Methods Appl. Mech. Engrg., 199 (2010), pp. 2765–2778.

[22] J. Shen, C. Wang, X. Wang, and S. M. Wise, *Second-order convex splitting schemes for gradient flows with Ehrlich–Schwoebel type energy: Application to thin film epitaxy*, SIAM J. Numer. Anal., 50 (2012), pp. 105–125, https://doi.org/10.1137/110822839.

[23] J. Shen and J. Xu, *Convergence and error analysis for the scalar auxiliary variable (SAV) schemes to gradient flows*, SIAM J. Numer. Anal., 56 (2018), pp. 2895–2912, https://doi.org/10.1137/17M1159968.

[24] J. Shen, J. Xu, and J. Yang, *The scalar auxiliary variable (SAV) approach for gradient flows*, J. Comput. Phys., 353 (2018), pp. 407–416.

[25] J. Shen, J. Xu, and J. Yang, *A new class of efficient and robust energy stable schemes for gradient flows*, SIAM Rev., 61 (2019), pp. 474–506, https://doi.org/10.1137/17M1150153.

[26] J. Shen and X. Yang, *Numerical approximations of Allen-Cahn and Cahn-Hilliard equations*, Discrete Contin. Dyn. Syst, 28 (2010), pp. 1669–1691.

[27] J. Shen, X. Yang, and H. Yu, *Efficient energy stable numerical schemes for a phase field moving contact line model*, J. Comput. Phys., 284 (2015), pp. 617–630.

[28] J. Shin, H. G. Lee, and J.-Y. Lee, *First and second order numerical methods based on a new convex splitting for phase-field crystal equation*, J. Comput. Phys., 327 (2016), pp. 519–542.

[29] C. Wang and S. M. Wise, *An energy stable and convergent finite-difference scheme for the modified phase field crystal equation*, SIAM J. Numer. Anal., 49 (2011), pp. 945–969, https://doi.org/10.1137/090752675.

[30] X. Wang, L. Ju, and Q. Du, *Efficient and stable exponential time differencing Runge-Kutta methods for phase field elastic bending energy models*, J. Comput. Phys., 316 (2016), pp. 21–38.

[31] A. A. Wheeler, W. J. Boettinger, and G. B. McFadden, *Phase-field model for isothermal phase transitions in binary alloys*, Phys. Rev. A, 45 (1992), pp. 7424–7439.

[32] A. A. Wheeler, B. T. Murray, and R. J. Schaefer, *Computation of dendrites using a phase field model*, Phys. D, 66 (1993), pp. 243–262.

[33] S. M. Wise, C. Wang, and J. S. Lowengrub, *An energy-stable and convergent finite-difference scheme for the phase field crystal equation*, SIAM J. Numer. Anal., 47 (2009), pp. 2269–2288, https://doi.org/10.1137/080738143.

[34] J. Xu, Y. Li, S. Wu, and A. Bousquet, *On the stability and accuracy of partially and fully implicit schemes for phase field modeling*, Comput. Methods Appl. Mech. Engrg., 345 (2019), pp. 826–853.

[35] X. Yang, *Linear, first and second-order, unconditionally energy stable numerical schemes for the phase field model of homopolymer blends*, J. Comput. Phys., 327 (2016), pp. 294–316.

[36] X. Yang, *Numerical approximations for the Cahn-Hilliard phase field model of the binary fluid-surfactant system*, J. Sci. Comput., 74 (2018), pp. 1533–1553.

[37] X. Yang and D. Han, *Linearly first-and second-order, unconditionally energy stable schemes for the phase field crystal model*, J. Comput. Phys., 330 (2017), pp. 1116–1134.

[38] X. Yang and L. Ju, *Efficient linear schemes with unconditional energy stability for the phase field elastic bending energy model*, Comput. Methods Appl. Mech. Engrg., 315 (2017), pp. 691–712.

[39] X. Yang and G. Zhang, *Numerical Approximations of the Cahn-Hilliard and Allen-Cahn Equations with General Nonlinear Potential Using the Invariant Energy Quadratization Approach*, preprint, https://arxiv.org/abs/1712.02760, 2017.

[40] X. Yang, J. Zhao, and Q. Wang, *Numerical approximations for the molecular beam epitaxial growth model based on the invariant energy quadratization method*, J. Comput. Phys., 333 (2017), pp. 104–127.

[41] J. Zhang and X. Yang, *On efficient numerical schemes for a two-mode phase field crystal model with face-centered-cubic (FCC) ordering structure*, Appl. Numer. Math., 146 (2019), pp. 13–37.

[42] J. Zhao, L. Chen, and H. Wang, *On power law scaling dynamics for time-fractional phase field models during coarsening*, Commun. Nonlinear Sci. Numer. Simul., 70 (2019), pp. 257–270.